

# Ways to constrain neutron star equation of state models using relativistic disc lines

Sudip Bhattacharyya<sup>\*</sup>

*Department of Astronomy and Astrophysics, Tata Institute of Fundamental Research, Mumbai 400005, India*

## ABSTRACT

Relativistic spectral lines from the accretion disc of a neutron star low-mass X-ray binary can be modelled to infer the disc inner edge radius. A small value of this radius tentatively implies that the disc terminates either at the neutron star hard surface, or at the innermost stable circular orbit (ISCO). Therefore an inferred disc inner edge radius either provides the stellar radius, or can directly constrain stellar equation of state (EoS) models using the theoretically computed ISCO radius for the spacetime of a rapidly spinning neutron star. However, this procedure requires numerical computation of stellar and ISCO radii for various EoS models and neutron star configurations using an appropriate rapidly spinning stellar spacetime. We have fully general relativistically calculated about 16000 stable neutron star structures to explore and establish the above mentioned procedure, and to show that the Kerr spacetime is inadequate for this purpose. Our work systematically studies the methods to constrain EoS models using relativistic disc lines, and will motivate future X-ray astronomy instruments.

**Key words:** accretion, accretion discs — equation of state — methods: numerical — relativity — stars: neutron — X-rays: binaries

## 1 INTRODUCTION

The core density of a neutron star is typically 5 – 10 times higher than the nuclear density. Such a dense matter at a relatively low temperature (e.g.,  $\sim 10^8$  K) cannot be probed by heavy-nuclei collision experiments or with observations of the early universe (Lattimer and Prakash (2007) and references therein). Plausibly the only way to probe this degenerate matter is to constrain the theoretically proposed equation of state (EoS) models of neutron star cores (Shapiro and Teukolsky 1983). For a given EoS model and an assumed central density, the stable structure of a non-spinning neutron star can be computed by solving the Tolman-Oppenheimer-Volkoff (TOV) equation (Shapiro and Teukolsky 1983). These stable stars trace a single curve in the mass ( $M$ ) – equatorial-radius ( $R$ ) space. Therefore, measurement of mass and radius of the same non-spinning neutron star would constrain the EoS models. If the neutron star spins, then the EoS models can be constrained by the reliable measurements of three independent parameters, such as mass, radius and spin-frequency ( $\nu_{\text{spin}}$ ) of the *same* neutron star (e.g., Fig. 1 of Bhattacharyya (2010)). This is extremely difficult because of a number of unknown systematics. Low-mass X-ray binaries (LMXBs) can be par-

ticularly promising systems for such measurements, because several complementary methods are available for them. A recent review by Bhattacharyya (2010) describes how the simultaneous application of these methods can reduce the systematic uncertainties.

One such method involves broad relativistic spectral lines from the inner portion of the accretion disc. The strongest among these fluorescent spectral emission lines is the one for the  $n = 2 \rightarrow n = 1$  transition of the iron atom (or ion), and is observed from many accreting supermassive and stellar-mass black hole systems (see Reynolds and Nowak (2003); Miller (2007); and references therein). Recently, Bhattacharyya and Strohmayer (2007) has, for the first time, established that the broad iron lines from neutron star LMXBs also originate from the inner accretion discs. This discovery was soon confirmed by Cackett et al. (2008) using data from a different satellite. After these initial reports, the inner disc origin of broad iron line has been confirmed for several other neutron star LMXBs (e.g., Pandel et al. (2008); D’Aí et al. (2009); Cackett et al. (2009); Papitto et al. (2009); Reis et al. (2009); di Salvo et al. (2009); Iaria et al. (2009); Cackett et al. (2010)).

The broad iron line is affected by the strong gravity and spin of the compact star (neutron star or black hole). Before discussing how this relativistic line can be used to

<sup>\*</sup> E-mail: sudip@tifr.res.in

constrain the neutron star parameters, let us see how it infers the black hole spin. The line shape, especially the extent of the red wing, carries the signature of the disc inner edge radius in the unit of stellar mass ( $r_{\text{in}}c^2/GM$ ). This is because the red wing is primarily affected by longitudinal Doppler effect due to the orbital motion of the disc matter, which broadens the line, and gravitational redshift, which shifts the line towards lower energies. Since, for a black hole the disc can extend up to the innermost stable circular orbit (ISCO), the black hole spin parameter  $j = Jc/GM^2$  ( $J$ : total angular momentum;  $M$ : mass), which determines the ISCO location, can be estimated by fitting the line shape with an appropriate relativistic model for Kerr spacetime (Laor 1991; Beckwith and Done 2004; Dovčiak et al. 2004; Miller 2007).

A neutron star system is usually more complex than a black hole system because of the following reasons. (1) While a spinning black hole is defined by only two parameters (mass and spin), and the spacetime around it is the Kerr spacetime having analytical expressions, the structures and spacetimes of rapidly spinning neutron stars, usually harboured by LMXBs, may have to be numerically calculated from at least two parameters apart from the EoS model (Cook et al. 1994). (2) Unlike a black hole, a neutron star has a hard surface which can have observable effects. Therefore, for a neutron star, the disc may be terminated either by ISCO or by the stellar surface (Thampan et al. 1999). An example of the competition between these two effects has been shown in the Fig. 1 of Miller et al. (1998) and Fig. 1 of Bhattacharyya et al. (2000), which demonstrate that usually circumferential radius  $r_{\text{in}}$  of disc inner edge first decreases and then increases with the increase of stellar spin for a given EoS model and mass. This complicates the measurement of  $Jc/GM^2$  and other stellar parameters using the inferred circumferential  $r_{\text{in}}c^2/GM$ , if it is not known whether the disc terminates at ISCO or at the stellar surface. Therefore, theoretical computations of  $r_{\text{in}}$  as a function of stellar parameters for various EoS models are essential. Such computations will also be useful to determine if a measured  $r_{\text{in}}c^2/GM$  directly gives the neutron star radius-to-mass ratio  $Rc^2/GM$ . Note that the computations of  $r_{\text{in}}$  and stellar parameters will involve the numerical calculations of rapidly spinning neutron star structures, and hence Kerr spacetime cannot be used. Moreover, in order to constrain the EoS models, directly measurable neutron star parameters (e.g.,  $Rc^2/GM$ ,  $M$ ,  $\nu_{\text{spin}}$ ; see Bhattacharyya (2010)) should be expressed as functions of  $r_{\text{in}}c^2/GM$ . Since  $Jc/GM^2$  cannot usually be measured directly, a  $Jc/GM^2$  vs.  $r_{\text{in}}c^2/GM$  plot may not be very useful to constrain the EoS models. In this paper, such plots (Figs 1, 2 and 3) have been shown for comparisons with Kerr spacetime and to gain insight (§ 3).

The procedure of constraining EoS models using directly measurable parameters vs.  $r_{\text{in}}c^2/GM$  relations can be utilized only if  $r_{\text{in}}c^2/GM \lesssim 6$ , because a much larger value of  $r_{\text{in}}c^2/GM$  might imply the truncation of the disc by other effects (see § 4). Particularly useful would be  $r_{\text{in}}c^2/GM < 6$ , because such values will confirm the effect of neutron star spin on a corotating disc. Therefore, a crucial question is whether observations show that  $r_{\text{in}}c^2/GM \lesssim 6$ . Cackett et al. (2010) report that  $r_{\text{in}}c^2/GM$  values fall into a small range of 6 – 15 for most of the neutron star LMXBs with established relativistic disc lines. Moreover, although

these authors could not measure a value of  $r_{\text{in}}c^2/GM$  less than 6 (as they used non-spinning, i.e., Schwarzschild spacetime), many of their fitted  $r_{\text{in}}c^2/GM$  values across the sources pegged at the lower limit 6. This happened for both phenomenological and reflection models, and even when the Compton broadening was taken into account (Cackett et al. 2010). Such pegged best-fit values strongly suggest that  $r_{\text{in}}c^2/GM < 6$  for many cases, which is supported by the disc line fitting with spinning Kerr spacetime models (Bhattacharyya and Strohmayer 2007; Papitto et al. 2009; Reis et al. 2009; D’Aí et al. 2010). This provides a good motivation to theoretically explore the above mentioned procedure to constrain the EoS models.

Since, in this paper, we have computed neutron star structures and the corresponding ISCO locations, let us briefly review some of the previous studies on this topic. Kluźniak and Wagoner (1985) computed ISCO location with slow stellar spin approximation. Cook et al. (1994) numerically calculated rapidly spinning neutron star structures in full general relativity using realistic EoS models. Miller et al. (1998) used these structure calculations to compute ISCO locations for a few cases. Stergioulas et al. (1999) studied if strange stars in LMXBs could be excluded using the orbital frequency at ISCO. The relevance of higher-order multipoles on the ISCO location was analytically probed by Shibata and Sasaki (1998). Berti and Stergioulas (2004) computed stellar models, multipole moments and ISCO locations, and compared the ISCO results with the Manko et al. (2000a,b) results for analytic solution for spacetime around rapidly spinning neutron stars, Kerr ISCO results and Shibata and Sasaki (1998) results. The results of Berti and Stergioulas (2004) show that higher multipole moments cause differences between rapidly spinning neutron star ISCO and Kerr ISCO. Pachon et al. (2006) and Sanabria-Gomez et al. (2010) studied the ISCO around a spinning magnetic neutron star. Abramowicz et al. (2003) calculated circular geodesics in the Hartle-Thorne metric for slowly spinning neutron stars. Berti et al. (2005) found that Hartle-Thorne approximation gives ISCO radii accurate to within 1%. Bejger et al. (2010) suggested approximate analytic expressions for circular orbits around rapidly spinning neutron stars.

Disc lines have so far been used to measure the black hole spin (e.g., Brenneman and Reynolds (2006)). It has also been proposed that these lines could be used to put an upper limit on the neutron star radius (Bhattacharyya and Strohmayer 2007; Cackett et al. 2008) and to constrain other stellar parameters (Bhattacharyya 2010). However, to the best of our knowledge, plausible methods to measure these parameters, and hence to constrain the EoS models in a systematic way using appropriate spacetimes have not been studied so far. The aim of this paper is to explore these methods. We have done so by calculating a huge number of neutron star structures, and the corresponding ISCO locations, if such a location is outside the neutron star. Although, a large set of papers reported the studies on such structures and locations (as indicated in the previous paragraph), none of these aimed to probe neutron star parameters using iron lines. In § 2, § 3 and § 4, we describe our method, give the results and provide a discussion respectively. Note that, since the accretion disc is believed to be thin, we have not considered

nonequatorial orbits in our calculations. We have also not considered counterrotating orbits, because that would imply  $r_{\text{ISCO}}c^2/GM > 6$ , which could be easily confused with truncations caused by other effects (see § 4).

## 2 METHOD

In this section, we briefly describe the procedure to compute rapidly spinning neutron star structures, and their equilibrium sequences. The spacetime around such a star can be described by the following metric (using  $c = G = 1$ ; Bardeen (1970); Cook et al. (1994)):

$$ds^2 = -e^{\gamma+\rho} dt^2 + e^{2\alpha} (dr^2 + r^2 d\theta^2) + e^{\gamma-\rho} r^2 \sin^2 \theta (d\phi - \omega dt)^2,$$

where the metric potentials  $\gamma$ ,  $\rho$ ,  $\alpha$ , and the angular speed ( $\omega$ ) of the stellar fluid relative to the local inertial frame are all functions of  $r$  and  $\theta$ . For a given EoS model, and assumed values of stellar central density and polar-radius to equatorial-radius ratio, Einstein's field equations can be solved to find out  $r$  and  $\theta$  dependence of  $\gamma$ ,  $\rho$ ,  $\alpha$  and  $\omega$ , as well as to obtain the stable stellar structure (Cook et al. 1994; Datta et al. 1998; Bhattacharyya et al. 2000, 2001a,b,c; Bhattacharyya 2002). This equilibrium solution can then be used to calculate bulk structure parameters (e.g.,  $M$ ,  $R$ ,  $J$ ) of the spinning neutron star. Note that, henceforth,  $R$  ( $= r_e e^{(\gamma_e - \rho_e)/2}$ ) will denote equatorial circumferential radius of the neutron star (equation B6 of Cook et al. (1994)). The equations of motion of a test particle in the spacetime around such a star are given in Thampan and Datta (1998). For example, the radial equation of motion is  $\dot{r}^2 \equiv e^{2\alpha+\gamma+\rho} (dr/d\tau)^2 = \tilde{E}^2 - \tilde{V}^2$ , where,  $d\tau$  is the proper time,  $\tilde{E}$  is the specific energy and a constant of motion, and  $\tilde{V}$  is the effective potential.  $\tilde{V}$  is given by  $\tilde{V}^2 = e^{\gamma+\rho} [1 + \frac{l^2/r^2}{e^{\gamma-\rho}}] + 2\omega\tilde{E}l - \omega^2 l^2$ , where  $l$  is the specific angular momentum, a constant of motion. We determine the radius of ISCO using the condition  $\tilde{V}_{,rr} = 0$ , where a comma followed by one  $r$  represents a first-order partial derivative with respect to  $r$  and so on (Thampan and Datta 1998). Thus we can compute both circumferential radius of ISCO (denoted by  $r_{\text{ISCO}}$ ) and  $R$ , and set the theoretical value of  $r_{\text{in}}$  to the larger of them (see § 1). For each EoS model, we have calculated  $\nu_{\text{spin}}$  sequences of equilibrium structures keeping  $\nu_{\text{spin}} = \text{constant}$ , and changing other parameters. Since  $\nu_{\text{spin}}$  is not an input for computing structures, a number of iterations are usually needed to compute the structure for a desired  $\nu_{\text{spin}}$  value. The other sequences (e.g.,  $M$  sequence,  $Rc^2/GM$  sequence; figures of § 3) have been calculated by interpolations of  $\nu_{\text{spin}}$  sequences.

We have used four representative EoS models of widely varying stiffness properties. This ensures sufficient generality of our results. We briefly describe these models below. *Model A* (Sahu et al. 1993): This very stiff EoS model with maximum non-spinning mass  $M_{\text{max}} \approx 2.59M_{\odot}$  is a field theoretical EoS for neutron-rich matter in beta equilibrium based on the chiral sigma model. *Model B* (Akmal et al. 1998): This stiff EoS model with  $M_{\text{max}} \approx 2.20M_{\odot}$  is the Argonne  $v_{18}$  model of two-nucleon interaction, with the three-nucleon interaction (Urbana IX [UIX] model) and the effect of relativistic boost corrections. *Model C* (Baldo et al. 1997): This intermediate EoS model with  $M_{\text{max}} \approx 1.79M_{\odot}$  is a microscopic EoS for asymmetric nuclear matter, derived

from the Brueckner-Bethe-Goldstone manybody theory with explicit three-body terms. *Model D* (Pandharipande 1971): This very soft EoS model with  $M_{\text{max}} \approx 1.41M_{\odot}$  assumes an admixture of hyperons with the hyperonic potentials similar to the nucleon-nucleon potentials, but altered suitably to represent the different isospin states.

## 3 RESULTS

We have computed  $\nu_{\text{spin}}$  sequences (§ 2) for 15  $\nu_{\text{spin}}$  values in the range of 0 – 750 Hz for each EoS model. About 16000 neutron star structures have been calculated to establish our results, and we give example figures in this section using a fraction of our computed numbers. The code to compute these structures and  $r_{\text{ISCO}}$  values is well tested (Datta et al. 1998; Thampan and Datta 1998; Bhattacharyya et al. 2000, 2001a,b,c; Bhattacharyya 2002). So far Kerr spacetime has been used to model the iron lines from spinning neutron star systems. Therefore, first we examine how our  $Jc/GM^2$  vs.  $r_{\text{in}}c^2/GM$  plot deviates from the corresponding Kerr curve, in order to find out if Kerr calculations for iron lines can give acceptable constraints on neutron star parameters. Fig. 1 shows when the equatorial radius of the neutron star is smaller than the ISCO radius, the deviation is relatively small, but is not negligible, depending on the values of  $\nu_{\text{spin}}$  and  $M$  and the chosen EoS model. But when the neutron star equatorial radius is larger than the ISCO radius (see, for example, Miller et al. (1998)), the deviation is large because stellar equatorial radius increases with the increase of  $\nu_{\text{spin}}$ , and such a situation does not occur for black holes (Kerr spacetime). For example, for the EoS model A, the stellar equatorial radius is greater than the ISCO radius for all  $\nu_{\text{spin}}$  values for  $M = 1.4M_{\odot}$ , and hence the deviation is always very large. However, for  $M = 2.0M_{\odot}$ , the stellar equatorial radius is less than the ISCO radius for smaller values of  $\nu_{\text{spin}}$  (Fig. 2). In this case, the curves for both EoS models A and B are closer to the Kerr curve compared to these curves for  $M = 1.4M_{\odot}$ . However, for  $M = 2.0M_{\odot}$ , stable neutron star structures do not exist for EoS models C and D. Therefore, from Fig. 1 and Fig. 2 we find that the deviation is more for (1) higher  $\nu_{\text{spin}}$ , (2) lower  $M$ , and (3) stiffer EoS models. The first two effects can also be seen in Fig. 1 of Miller et al. (1998). These effects are expected for  $r_{\text{in}}c^2/GM = Rc^2/GM$ , because all these three points result in the increase of  $R$ . Let us now try to understand these points for  $r_{\text{in}}c^2/GM = r_{\text{ISCO}}c^2/GM$ . The first point is understandable, because for  $\nu_{\text{spin}} = 0$  the spacetime outside even a neutron star is Schwarzschild, which is the non-spinning special case of Kerr. The second point could be understood from the fact that for lower  $M$  the neutron star is usually less compact (that is the hard surface is farther from the centre), causing its spacetime to deviate more from that of a black hole. The third point may be explained from the lesser stellar compactness for a stiffer EoS model for given  $M$  and  $\nu_{\text{spin}}$ . However, we find that if  $M/M_{\text{max}}$  is kept fixed instead of  $M$ , the differences among the  $Jc/GM^2$  vs.  $r_{\text{in}}c^2/GM$  curves for various EoS models are small (Fig. 3). This indicates that  $M_{\text{max}}$  may be a suitable parameter to characterize an EoS model.

After finding that the Kerr spacetime is usually not good enough to model  $r_{\text{in}}c^2/GM$ , and since this spacetime

cannot be used for neutron star parameter calculation, we have explored ways to constrain stellar EoS models using appropriate general relativistic computations for neutron stars (see § 2). We have checked the relation between  $r_{\text{in}}c^2/GM$  and a few stellar parameters, which can be measured from independent methods. These parameters are  $\nu_{\text{spin}}$ ,  $Rc^2/GM$  and  $M$ . Whenever  $\nu_{\text{spin}}$  can be measured (using regular pulsations or burst oscillations; Bhattacharyya (2010)), it is measured very accurately. Therefore, in the Figs. 4, 5, 6 and 7, we have fixed  $\nu_{\text{spin}}$ .  $Rc^2/GM$  and  $M$ , on the other hand, may be constrained in a range (using thermonuclear X-ray bursts, binary orbital motions, etc.; Bhattacharyya (2010)), and hence we have used them as dependent variables in these figures. Figs. 4 and 5 show  $Rc^2/GM$  vs.  $r_{\text{in}}c^2/GM$  plots for two values of  $\nu_{\text{spin}}$  and four EoS models. For a given  $\nu_{\text{spin}}$  value, and if the stellar equatorial radius is less than the ISCO radius, each EoS model traces a distinct curve. These curves, which are more separated from each other for higher  $\nu_{\text{spin}}$ , can be used to constrain EoS models from the  $r_{\text{in}}c^2/GM$  value inferred from the iron line fitting, and the  $Rc^2/GM$  value measured independently (see Bhattacharyya (2010)). These figures show that even if  $Rc^2/GM$  is not well constrained, a suitable upper limit of  $r_{\text{in}}c^2/GM$  can reject softer EoS models. If the stellar equatorial radius is larger than the ISCO radius, an oblique straight line is found for all EoS models, and an inferred  $r_{\text{in}}c^2/GM$  value directly gives the  $Rc^2/GM$  value. Figs. 4 and 5 clearly show the value of  $r_{\text{in}}c^2/GM$  (for a given  $\nu_{\text{spin}}$ ), above which  $r_{\text{in}}c^2/GM$  can be used to directly infer the EoS-model-independent  $Rc^2/GM$  value. Figs. 6 and 7 show even if, instead of  $Rc^2/GM$ ,  $M$  is known from independent measurement (Bhattacharyya 2010),  $r_{\text{in}}c^2/GM$  inferred from iron line can be used to constrain the EoS models. Even for an unknown  $M$ , a suitable upper limit of  $r_{\text{in}}c^2/GM$  can be used to reject softer EoS models. Fig. 8 explores how for a known  $M$  value,  $r_{\text{in}}c^2/GM$  inferred from iron line and independently constrained  $Rc^2/GM$  can be used to constrain EoS models. Similar result is shown in Fig. 9, where  $Rc^2/GM$  is known and  $M$  is reasonably constrained. However, for these two procedures (Figs. 8 and 9), measurements of  $Rc^2/GM$  and  $M$  appear to be more important than an inferred  $r_{\text{in}}c^2/GM$ .

#### 4 DISCUSSION

In this paper, we explore ways to constrain neutron star EoS models by comparing the inferred values of  $r_{\text{in}}c^2/GM$  with the theoretical values. A  $r_{\text{in}}c^2/GM$  value may be inferred by fitting the relativistic disc lines with appropriate models (Bhattacharyya 2010). We have shown that  $r_{\text{in}}c^2/GM$  calculated from Kerr spacetime is inadequate to distinguish between EoS models even when  $r_{\text{in}}c^2/GM = r_{\text{ISCO}}c^2/GM$ , and can largely differ from the correct value for rapidly spinning neutron star spacetime when  $r_{\text{in}}c^2/GM = Rc^2/GM$ . We have numerically computed a huge number of  $r_{\text{in}}c^2/GM$  values, assuming that the disc terminates either at ISCO or at the stellar hard surface. This should be at least approximately true for  $r_{\text{in}}c^2/GM \lesssim 6$ , although systematics may be introduced due to the effects of magnetic field and radiative pressure. Such systematics would imply that any inferred  $r_{\text{in}}c^2/GM$  value is basically an upper limit of  $r_{\text{ISCO}}c^2/GM$

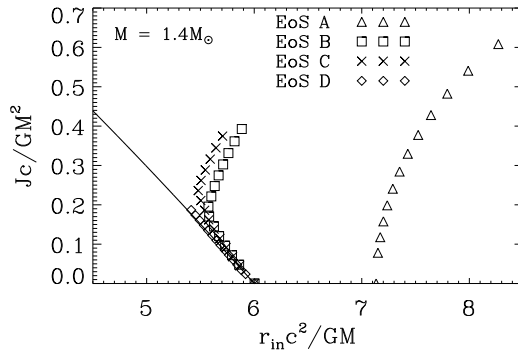


**Figure 1.** Neutron star angular momentum parameter ( $Jc/GM^2$ ) vs. disc inner edge radius to stellar mass ratio ( $r_{\text{in}}c^2/GM$ ). The solid curve is for Kerr spacetime (§ 1). Various symbols give the curves for different neutron star EoS models (§ 2) for  $M = 1.4M_{\odot}$ , and  $\nu_{\text{spin}}$  ranging from 0 Hz to 750 Hz. The negative slope of the curves implies that the disc terminates at ISCO, while the positive slope implies that it terminates at the stellar surface. This figure shows that the realistic  $r_{\text{in}}c^2/GM$  values for neutron stars can significantly deviate from the Kerr values.

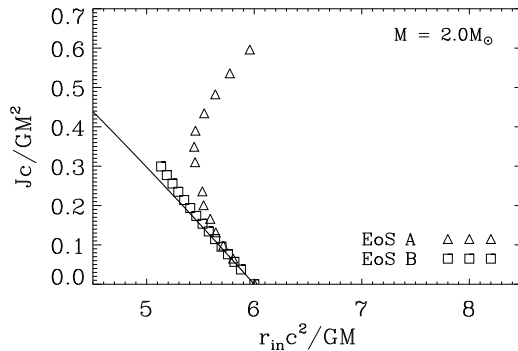


**Figure 2.** Neutron star angular momentum parameter ( $Jc/GM^2$ ) vs. disc inner edge radius to stellar mass ratio ( $r_{\text{in}}c^2/GM$ ). Similar to Fig. 1, but for  $M = 2.0M_{\odot}$ . Note that stable neutron star structures do not exist for this high mass for the softer equation of state models C and D (§ 2).

or  $Rc^2/GM$ , which can still be used to reject softer EoS models (Figs. 4, 5, 6 and 7). These systematics can be reduced by detailed modelling of these effects, as well as by independent observations. We have studied the relations between  $r_{\text{in}}c^2/GM$  and several directly measurable neutron star parameters (Bhattacharyya 2010), in order to establish new ways to constrain EoS models. We have found that this iron line method could be effective to constrain EoS models, if the neutron star spin frequency is independently measured (Bhattacharyya 2010). This work is timely and important, as it provides motivation for future X-ray missions, and because of the rapid progress in the disc line field via observations with *XMM-Newton*, *Suzaku* and *Chandra*.

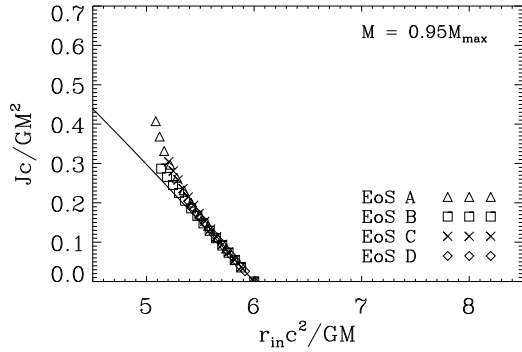


**Figure 3.** Neutron star angular momentum parameter ( $Jc/GM^2$ ) vs. disc inner edge radius to stellar mass ratio ( $r_{\text{in}}c^2/GM$ ). Similar to Fig. 1, but for  $M = 0.95 \times M_{\text{max}}$ . Here  $M_{\text{max}}$  is the maximum mass for a non-spinning stable neutron star for a given EoS. This figure shows that a fixed  $M/M_{\text{max}}$  gives similar curves, and hence  $M_{\text{max}}$  may be a suitable parameter to characterize an EoS model.

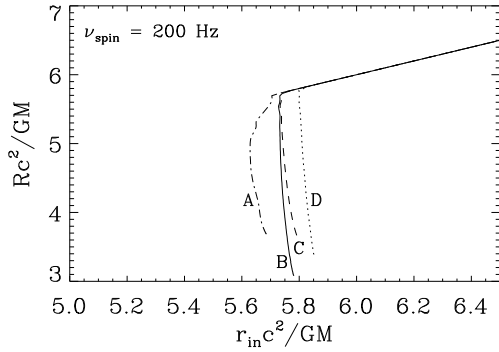


**Figure 4.** Neutron star equatorial-radius-to-mass ratio ( $Rc^2/GM$ ) vs. disc inner edge radius to stellar mass ratio ( $r_{\text{in}}c^2/GM$ ) for various EoS models (§ 2) for  $\nu_{\text{spin}} = 200$  Hz. Note that the oblique straight line portions of the curves are for  $r_{\text{in}}c^2/GM = Rc^2/GM$ . This figure shows how a  $r_{\text{in}}c^2/GM$  value inferred from iron line can be used to constrain the EoS models for a known  $\nu_{\text{spin}}$  value (§ 3).

## ACKNOWLEDGMENTS

We thank A. Thampan for the rapidly spinning neutron star structure computation code, and A. Gopakumar and B. Iyer for discussion. This work was supported in part by US NSF grant AST 0708424.

## REFERENCES

- Abramowicz M.A., Almergren G.J.E., Kluźniak W., Thampan, A.V., 2003, arXiv:gr-qc/0312070  
 Akmal A., Pandharipande V.R., Ravenhall D.G., 1998, Physical Review C, 58, 1804  
 Baldo M., Bombaci I., Burgio G.F., 1997, A&A, 328, 274  
 Bardeen J.M., 1970, ApJ, 162, 71  
 Beckwith K., Done C., 2004, MNRAS, 352, 353  
 Bejger M., Zdunik J.L., Haensel P., 2010, A&A, 520, 16

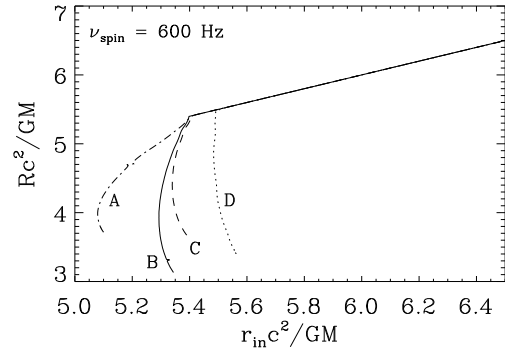


**Figure 5.** Neutron star equatorial-radius-to-mass ratio ( $Rc^2/GM$ ) vs. disc inner edge radius to stellar mass ratio ( $r_{\text{in}}c^2/GM$ ) for various EoS models (§ 2) for  $\nu_{\text{spin}} = 600$  Hz (similar to Fig. 4).

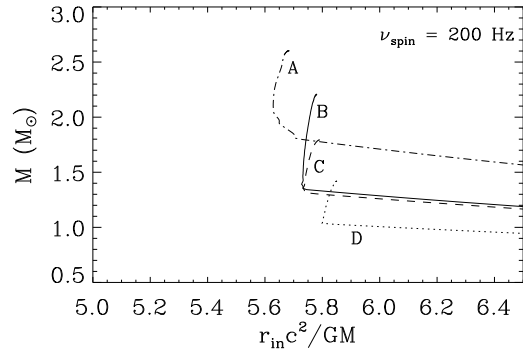


**Figure 6.** Neutron star mass ( $M$ ) vs. disc inner edge radius to stellar mass ratio ( $r_{\text{in}}c^2/GM$ ) for various EoS models (§ 2) for  $\nu_{\text{spin}} = 200$  Hz. Note that the oblique straight line portions of the curves are for  $r_{\text{in}}c^2/GM = Rc^2/GM$ . This figure shows how a  $r_{\text{in}}c^2/GM$  value inferred from iron line can be used to constrain the EoS models for a known  $\nu_{\text{spin}}$  value (§ 3).

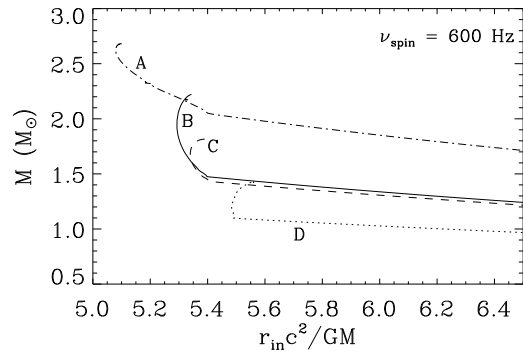


**Figure 7.** Neutron star mass ( $M$ ) vs. disc inner edge radius to stellar mass ratio ( $r_{\text{in}}c^2/GM$ ) for various EoS models (§ 2) for  $\nu_{\text{spin}} = 600$  Hz (similar to Fig. 6).

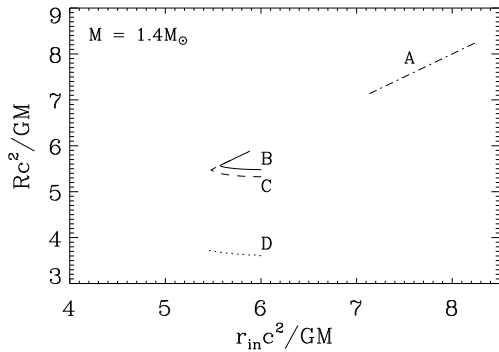


**Figure 8.** Neutron star equatorial-radius-to-mass ratio ( $Rc^2/GM$ ) vs. disc inner edge radius to stellar mass ratio ( $r_{in}c^2/GM$ ) for various EoS models (§ 2) for  $M = 1.4M_{\odot}$ . Note that the oblique straight line portions of the curves are for  $r_{in}c^2/GM = Rc^2/GM$ . This figure shows, for a known  $M$ , how a  $r_{in}c^2/GM$  value inferred from iron line can be used to constrain the EoS models (§ 3).

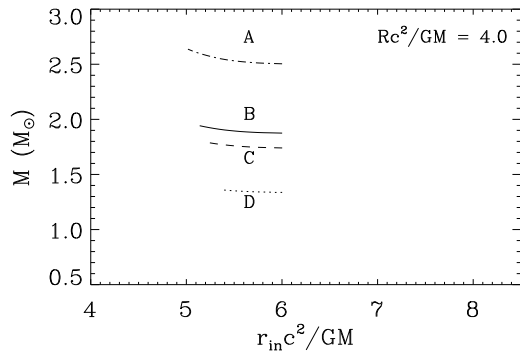


**Figure 9.** Neutron star mass ( $M$ ) vs. disc inner edge radius to stellar mass ratio ( $r_{in}c^2/GM$ ) for various EoS models (§ 2) for  $Rc^2/GM = 4.0$ . This figure shows, for a known  $Rc^2/GM$ , how a  $r_{in}c^2/GM$  value inferred from iron line can be used to constrain the EoS models (§ 3).

Berti E., Stergioulas N., 2004, MNRAS, 350, 1416  
 Berti E., White F., Maniopolou A., Bruni M., 2005, MNRAS, 358, 923  
 Bhattacharyya S., 2002, A&A, 383, 524  
 Bhattacharyya S., 2010, Advances in Space Research, 45, 949  
 Bhattacharyya S., Bhattacharya D., Thampan A.V., 2001, MNRAS, 325, 989  
 Bhattacharyya S., Misra R., Thampan A.V., 2001, ApJ, 550, 841  
 Bhattacharyya S., Strohmayer T.E., 2007, ApJ, 664, L103  
 Bhattacharyya S., Thampan A.V., Bombaci I., 2001, A&A, 372, 925  
 Bhattacharyya S., Thampan A.V., Misra R., Datta B., 2000, ApJ, 542, 473  
 Brenneman L.W., Reynolds C.S., 2006, ApJ, 652, 1028  
 Cackett E.M., Altamirano D., Patruno A., et al., 2009, ApJ, 694, L21

Cackett E.M., Miller J.M., Ballantyne D.R., et al., 2010, ApJ, 720, 205  
 Cackett E.M., Miller J.M., Bhattacharyya S., et al., 2008, ApJ, 674, 415  
 Cook G.B., Shapiro S.L., Teukolsky S.A., 1994, ApJ, 424, 823  
 D'Aí A., di Salvo T., Ballantyne D., et al., 2010, A&A, 516, 36  
 D'Aí A., Iaria R., Di Salvo T., Matt G., Robba N.R., 2009, ApJ, 693, L1  
 Datta B., Thampan A.V., Bombaci I., 1998, A&A, 334, 943  
 di Salvo T., D'Aí A., Iaria R., et al., 2009, MNRAS, 398, 2022  
 Dovčiak M., Karas V., Yaqoob T., 2004, ApJSS, 153, 205  
 Iaria R., D'Aí A., Di Salvo T., et al., 2009, A&A, 505, 1143  
 Kluźniak W., Wagoner R.V., 1985, ApJ, 297, 548  
 Laor A., 1991, ApJ, 376, 90  
 Lattimer J.M., Prakash M., 2007, Physics Reports, 442, 109  
 Manko V.S., Mielke E.W., Sanabria-Gómez J.D., 2000a, Phys. Rev. D, 61, 081501  
 Manko V.S., Sanabria-Gómez J.D., Manko O.V., 2000b, Phys. Rev. D, 62, 044048  
 Miller J.M., 2007, ARA&A, 45, 441  
 Miller M.C., Lamb F.K., Cook G.B., 1998, ApJ, 509, 793  
 Pachon L.A., Rueda J.A., Sanabria-Gómez J.D., 2006, Phys. Rev. D, 73, 104038  
 Pandel D., Kaaret P., Corbel S., 2008, ApJ, 688, 1288  
 Pandharipande V.R., 1971, Nucl. Phys., A178, 123  
 Papitto A., Di Salvo T., D'Aí A., Iaria R., Burderi L., Riggio A., Menna M.T., Robba, N.R., 2009, A&A, 493, L39  
 Reis R.C., Fabian A.C., Young A.J., 2009, MNRAS, 399, L1  
 Reynolds C.S., Nowak M.A., 2003, Physics Reports, 377, 389  
 Sahu P.K., Basu R., Datta B., 1993, ApJ, 416, 267  
 Sanabria-Gómez J.D., Hernández-Pastora J.L., Dubeibe F.L., 2010, Phys. Rev. D, 82, 124014  
 Shapiro S.L., Teukolsky S.A., 1983, Black Holes, White Dwarfs, and Neutron Stars: The Physics of Compact Objects, John Wiley & Sons (New York)  
 Shibata M., Sasaki M., 1998, Phys. Rev. D, 58, 104011  
 Stergioulas N., Kluźniak W., Bulik T., 1999, A&A, 352, L116  
 Thampan A.V., Bhattacharya D., Datta B., 1999, MNRAS, 302, L69  
 Thampan A.V., Datta, B., 1998, MNRAS, 297, 570